Supporting Information

Carpenito *et al.* 10.1073/pnas.0813101106

SI Materials and Methods

Generation of Antimesothelin T-Body Molecules. The anti-mesothelin scFv (SS1)-PE38 (1) was used as a template for PCR amplification of an 850-bp SS1 fragment using the following primers: 5′-TGCCGCTGGCCTTGCTGCTCCACGCCGC-CAGGCCGGGATCCCAGGTACAACTGCAGCAGTC-3′ (BamH*I* is underlined) and 5′-GGTCGCGGCGCTG-GCGTCGTGGTGCTAGCTTTGATTTCCAACTTTGT-CCCAGC-3′ (Nhe*I* is underlined). The resulting PCR product contained a BamH*I* site on the 5′ end and an Nhe*I* site on the 3′ end. The CD8α hinge, transmembrane, and cytosolic regions were amplified by PCR using previously constructed templates and the following primers 5′- GCTGGGACAAAGTTGGA-AATCAAAGCTAGCACCACGACGCCAGCGCCGCGACC-3′ (Nhe*I* is underlined) and either 5′-TCGACAGTCGACTTAGC-GAGGGGGCAGGGCCT-3′ (for the functional TCRζ containing molecules, Sal*I* is underlined) or 5′-TCGACAGTCGACT-TACGCGGGGGCGTCTGCGCTCC-3′ (for the truncated CD3 ζ construct, Sal*I* is underlined). The chimeric immunoreceptor constructs were generated through gene splicing by overlap extension. Equimolar amounts of the SS1 PCR product and CD8 hinge, transmembrane, and cytosolic PCR products were combined with 5′-ATAGCATCTAGAATGGCCTTACCAGTGACC-GCCTTGCTCCTGCCGCTGGCCTTGCTGCTC-3′ (Xba*I* is underlined) and either 5′-TCGACAGTCGACTTAGCGA-GGGGGCAGGGCCT-3′(for the functional CD3ζ containing molecules, Sal*I* is underlined) or 5′-TCGACAGTCGACT-TACGCGGGGGCGTCTGCGCTCC-3′(for the truncated CD3ζ construct, Sal*I* is underlined). The final PCR products were then digested with XbaI and SalI and ligated into pELNS, third-generation self-inactivating lentiviral expression vectors based on pRRL-SIN-CMV-eGFP-WPRE (2), in which transgene expression is driven by the EF-1α promoter. High-titer replication-defective lentiviral vectors were produced and concentrated as previously described (3).

Cell Lines. The human erythroleukemic cell line K562 and the human epidermoid carcinoma cell line A431 were maintained in RPMI 1640 supplemented with 10% FCS, 100 U/ml penicillin, 100-μg/ml streptomycin sulfate, and 10-mM Hepes. Mesothelin-expressing K562 and A431 cells were generated by transducing with a mesothelin-encoding lentiviral vector (a generous gift from Dr. Elizabeth Jaffee). Transduced cells expressing high levels of mesothelin were collected using a MOFLO cell sorter (Cytomation), and cultured as described above. The generation and propagation of ovarian cancer cell lines OvCa61.4 and OvCa68.4 has been previously described (4), and mesothelioma cell line M108 was derived from a malignant pleural effusion obtained from a mesothelioma patient using identical techniques. In addition to establishing a cell line, multiple aliquots of primary pleural effusion cells from this patient were cryopreserved and used as described below. All patient specimens were obtained under University of Pennsylvania Institutional Review Board-approved protocols.

Animals. All animal experiments were approved by the University of Pennsylvania Institutional Animal Care and Use Committee. NOD/*scid*/*IL2r*$\gamma^{-/-}$ (NOG) (5) mice were purchased from the Jackson Laboratory. C57BL/6J x C57BL/10SgSnAi)-[KO]γc-[KO]Rag2 mice (Rag2$\gamma^{-/-}$) were purchased from Taconic Farms (6). Animals were also bred in the Animal Services Unit of the University of Pennsylvania. The mice were housed under specific pathogen-free conditions in microisolator cages and given unrestricted access to autoclaved food and acidified water. Animals of both sexes were used for experiments at 10 to 16 weeks of age. Two-week prophylactic antibiotic treatment (1-mg/ml neomycin sulfate and 200-U/ml polymyxin sulfate in drinking water) was initiated following tumor-cell injections.

Antibodies. The following conjugated antibodies were purchased from BD Biosciences: mouse IgG1 isotype, goat anti-mouse Ig (PE), anti-CD4 (FITC), anti-CD4 (PerCP-Cy5.5), anti-CD8 (APC), anti-CD8 (APC-H7), anti-CD45 (PE), anti-TNF-α (PE-Cy7), and anti-IFN-γ (V450). Anti-IL-2 (Alexa Fluor 488) antibody was purchased from Biolegend. Anti-GM-CSF (Alexa Fluor 647) antibody was purchased from eBiosciences. The anti-Bcl-X_L (PE) antibody was purchased from Southern Biotech. The anti-human mesothelin antibody CAK1 was purchased from Signet Laboratories. The biotinylated F(ab′)$_2$ fragment of goat anti-mouse IgG sera (specific for scFvs of murine origin) was purchased from Jackson ImmunoResearch. Streptavidin (PE) and streptavidin (PE-TexasRed) were purchased from BD Biosciences. To visualize tumor mesothelin expression, animals were killed, and excised tumors were embedded in OCT medium and stained with the CAK1 antibody followed by biotinylated secondary antibody (goat anti-mouse IgG; Vectastain Elite ABC kit). Signal was localized using 3,3′-diaminobenzidine tetrahydrochloride as the chromogen.

Isolation, Transduction, and Expansion of Primary Human T Lymphocytes. Primary human CD4$^+$ T and CD8+ T cells were isolated from healthy volunteer donors following leukapheresis by negative selection using RosetteSep kits (Stem Cell Technologies). All specimens were collected under a University Institutional Review Board-approved protocol, and written informed consent was obtained from each donor. T cells were cultured in RPMI 1640 supplemented with 10% FCS, 100-U/ml penicillin, 100-μg/ml streptomycin sulfate, 10-mM Hepes, and stimulated with magnetic beads coated with anti-CD3/anti-CD28 at a 1:3 cell to bead ratio. For CD8+ T cells, human IL-2 (Chiron) was added every other day to a final concentration of 30 IU/ml. Approximately 24 h after activation, T cells were transduced with lentiviral vectors at an MOI of $\approx$5. CD4$^+$ and CD8+ T cells used for in vivo experiments and intracellular cytokine stains were mixed at 1:1 ratio, activated, and transduced as described above (without the addition of exogenous IL-2). Cells were counted and fed every 2 days and once T cells appeared to rest down, as determined by both decreased growth kinetics and cell size, they were either used for functional assays or cryopreserved.

Flow Cytometric Analysis. K562, K562.meso, A431.meso, OvCa61.4, OvCa68.4, and M108 cells were stained for surface expression of mesothelin using the CAK1 antibody followed by PE-labeled secondary antibodies. Expression of the various SS1 scFv fusion proteins on T cells was detected using biotinylated goat anti-mouse IgG followed by staining with either streptavidin (PE) or streptavidin (PE-TexasRed). Samples were analyzed on either LSRII or FACSCalibur flow cytometers (BD Biosciences) and analyzed with FlowJo software (TreeStar).

Chromium Release Assay. Target cells were loaded with ^{51}Cr and combined with differing amounts of transduced CD8+ T cells in V-bottom plates. After a 4-h incubation at 37 °C, the release of free ^{51}Cr was measured using a COBRA II automated gamma-

counter (Packard Instrument Company). The percent-specific lysis was calculated using the formula: % specific lysis = 100 $\times$ (experimental cpm release – spontaneous cpm release)/(total cpm release – spontaneous cpm release). All data are represented as a mean of triplicate wells (+/– SD).

Cytokine Production and Intracellular Staining of Restimulated T Cells. Cryopreserved T cells transduced with SS1 fusion proteins were thawed, washed, and placed in culture for ≈8 to 10 h. T cells (1×10^6) were cocultured with 5×10^5 irradiated (100 Gy) K562, K562.meso, or M108 cells and supernatants were harvested 24 h later. Concentrations of IL-2, IL-6, IFN-γ, and TNF-α were determined using the Human Th1/Th2 Cytokine Kit II (BD Biosciences). Intracellular cytokine production was measured under identical culture conditions, except that GolgiStop (BD Biosciences) was added either after 1 h or 16 h of coculture. Cells were then cultured for an additional 4 h. Cultures were stained for SS1 scFvs, followed by CD4 and CD8. Permeabilized cells were then stained intracellularly for IFN-γ, TNF-α, IL-2, and GM-CSF production. Similar conditions in the absence of GolgiStop were also examined for intracellular Bcl-X_L expression. T cells were gated on CD4 and CD8 expression and further analyzed for cytokine expression using a Boolean gate platform to assess all of the possible patterns of cytokine responses.

Statistical Analysis. All results were expressed as means ± SD or SEM, as indicated. Tumor volume data were transformed to the log scale before analysis. We analyzed the tumor growth data with regression spline models (7). Specifically, we modeled the data in all 7 treatment groups with a common quadratic curve in the period before T cell transfer, and with separate linear and quadratic coefficients (by treatment group) in the period after T cell transfer. To test for differences between treatment groups, we tested whether the posttransfer linear and quadratic coefficients were equal. We fit the curves using mixed models (Proc Mixed, SAS Institute, Inc.) to account for correlation within animals. To examine the persistence of T cells in circulation, we analyzed CD4 and CD8 counts measured on day 73 after tumor implant. Because SDs were generally larger for groups with larger means, we transformed the cell counts to the log scale, which rendered distributions more nearly normal with roughly equal SDs in all 7 treatment groups. We then analyzed the data by analysis of variance (Proc GLM, SAS Institute, Inc.), applying the Tukey correction for multiplicity in pairwise comparisons of means. We applied an identical analysis to data on T-cell engraftment as a function of route of administration.

SI Discussion. Our study suggests that in vitro experiments can be misleading in predicting the efficacy of the engineered T cells in vivo. For example, we observed that T cells expressing TCRζ were sufficient for in vitro killing of tumor; however, in vivo, only T cells endowed with costimulatory receptors were able to control pre-established tumors. T cells expressing CD137 domains were favored for engineering T cells to be multifunctional cytokine-secreting cells. Finally, none of the in vitro studies clearly indicated that cells expressing the tripartite CD28, CD137, and TCRζ signaling domains would have the most potent antitumor effects in vivo. However, the T cells expressing the tripartite vector had the highest levels of persistence in vivo, perhaps confirming other studies suggesting that engraftment and persistence of adoptively transferred T cells is a surrogate biomarker that is necessary for in vivo tumor eradication (8, 9).

Engineered cells expressing the CD137 signaling domain were more likely to be multifunctional and persist in tumor-bearing mice. Given that multifunctional cells correlate with central memory cells (10), this may explain why cells containing redirected T cells with the CD137 domain were more effective for tumor therapy in vivo, because previous studies have shown that central memory cells are more effective for adoptive immunotherapy (11). Others have shown that CD137 is more effective than CD28 at expanding tumor-specific human CD8 T cells in vitro (12). We were surprised to observe that the CD137 domain did not drive the expression of Bcl-X_L, because previous studies of natural T cells stimulated with antigen-presenting cells engineered to express CD137 found that Bcl-X_L was expressed in the stimulated T cells (13). However, as noted above, other evidence from our studies indicates that inclusion of the CD137 domain was beneficial, as cells endowed with CD137 were more likely multifunctional and persisted longer in tumor-bearing mice. Furthermore, our findings suggest that incorporation of the CD137 intracellular domain mediates an antigen-independent survival effect that is similar to that provided by the natural 4–1BB receptor in T cells following ligation (14, 15).

1. Chowdhury PS, Viner JL, Beers R, Pastan I (1998) Isolation of a high-affinity stable single-chain Fv specific for mesothelin from DNA-immunized mice by phage display and construction of a recombinant immunotoxin with anti-tumor activity. *Proc Natl Acad Sci USA* 95:669–674.
2. Dull T, *et al.* (1998) A third-generation lentivirus vector with a conditional packaging system. *J Virol* 72:8463–8471.
3. Parry RV, *et al.* (2003) CD28 and inducible costimulatory protein Src homology 2 binding domains show distinct regulation of phosphatidylinositol 3-kinase, Bcl-xL, and IL-2 expression in primary human CD4 T lymphocytes. *J Immunol* 171:166–174.
4. Bertozzi CC, *et al.* (2006) Multiple initial culture conditions enhance the establishment of cell lines from primary ovarian cancer specimens. *In Vitro Cell Dev Biol Anim* 42:58–62.
5. Shultz LD, *et al.* (2005) Human lymphoid and myeloid cell development in NOD/LtSz-scid IL2R gamma null mice engrafted with mobilized human hemopoietic stem cells. *J Immunol* 174:6477–6489.
6. Garcia S, DiSanto J, Stockinger B (1999) Following the development of a CD4 T cell response in vivo: from activation to memory formation. *Immunity* 11:163–171.
7. Durrleman S, Simon R (1989) Flexible regression models with cubic splines. *Stat Med* 8:551–561.
8. Greenberg PD, Cheever MA (1984) Treatment of disseminated leukemia with cyclophosphamide and immune cells: tumor immunity reflects long-term persistence of tumor-specific donor T cells. *J Immunol* 133:3401–3407.
9. Zhou J, *et al.* (2005) Telomere length of transferred lymphocytes correlates with in vivo persistence and tumor regression in melanoma patients receiving cell transfer therapy. *J Immunol* 175:7046–7052.
10. Appay V, Douek DC, Price DA (2008) CD8+ T cell efficacy in vaccination and disease. *Nat Med* 14:623–628.
11. Klebanoff CA, *et al.* (2005) Central memory self/tumor-reactive CD8+ T cells confer superior antitumor immunity compared with effector memory T cells. *Proc Natl Acad Sci USA* 102:9571–9576.
12. Zhang H, *et al.* (2007) 4–1BB is superior to CD28 costimulation for generating CD8+ cytotoxic lymphocytes for adoptive immunotherapy. *J Immunol* 179:4910–4918.
13. Bukczynski J, *et al.* (2004) Costimulatory ligand 4–1BBL (CD137L) as an efficient adjuvant for human antiviral cytotoxic T cell responses. *Proc Natl Acad Sci USA* 101:1291–1296.
14. Pulle G, Vidric M, Watts TH (2006) IL-15-dependent induction of 4–1BB promotes antigen-independent CD8 memory T cell survival. *J Immunol* 176:2739–2748.
15. Zhu Y, *et al.* (2007) CD137 stimulation delivers an antigen-independent growth signal for T lymphocytes with memory phenotype. *Blood* 109:4882–4889.

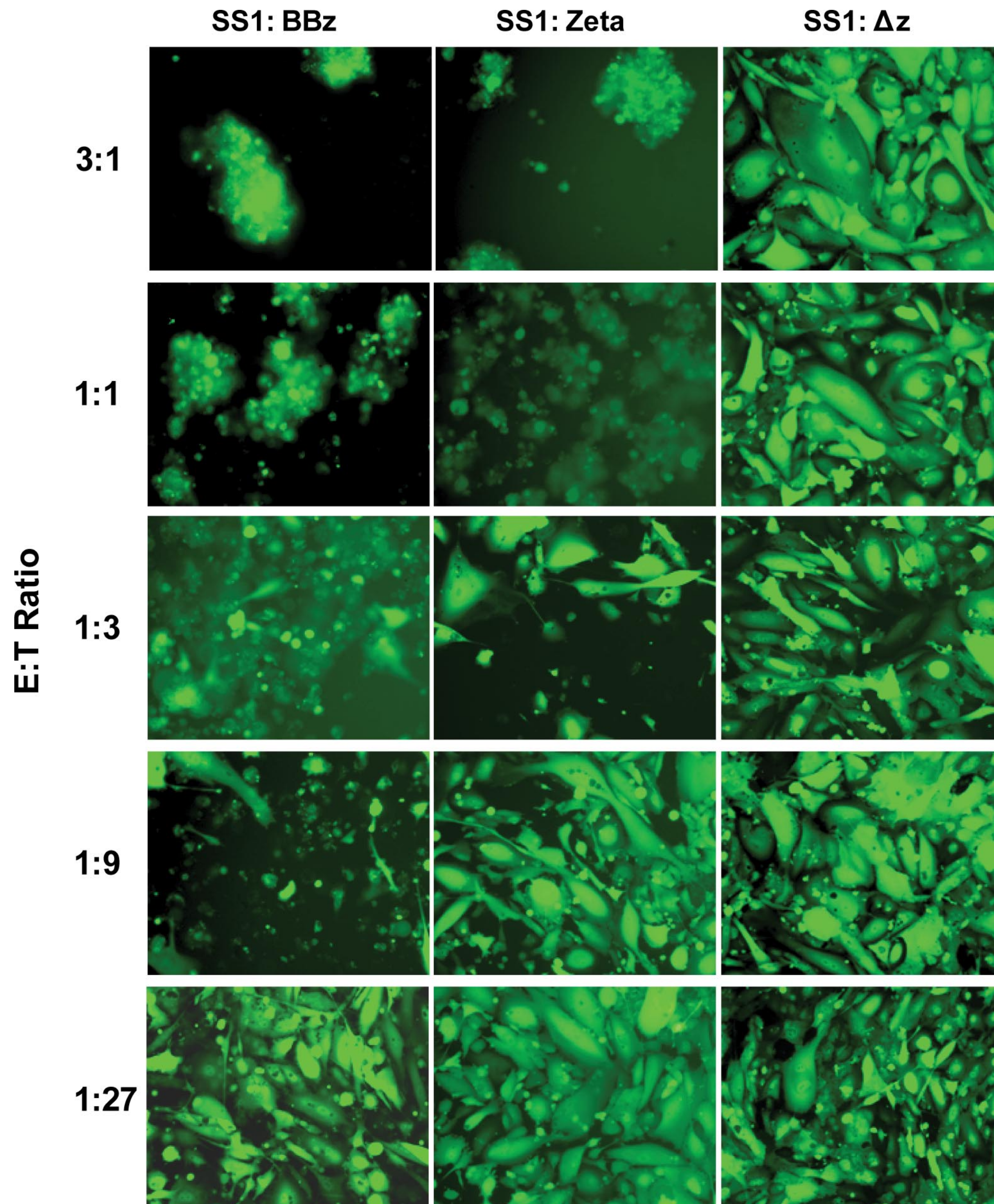

Fig. S1. Efficient mesothelin-specific killing of M108 tumor cells in vitro. M108 cells (1×10^6) transduced with GFP were grown for 36 h before the addition of decreasing numbers (3×10^6, 1×10^6, 3×10^5, 1×10^5, and 3×10^4 cells) of SS1-CIR transduced CD8+ T cells; the transduction efficiencies for each group were: SS1-BBz 32%, SS1-Zeta 45%, and SS1-Δz 53%. Cultures were allowed to progress for an additional 48 h, after which cells were photographed under fluorescence microscopy. The nominal E:T ratio is indicated (i.e., ratios were not corrected for transduction efficiency).

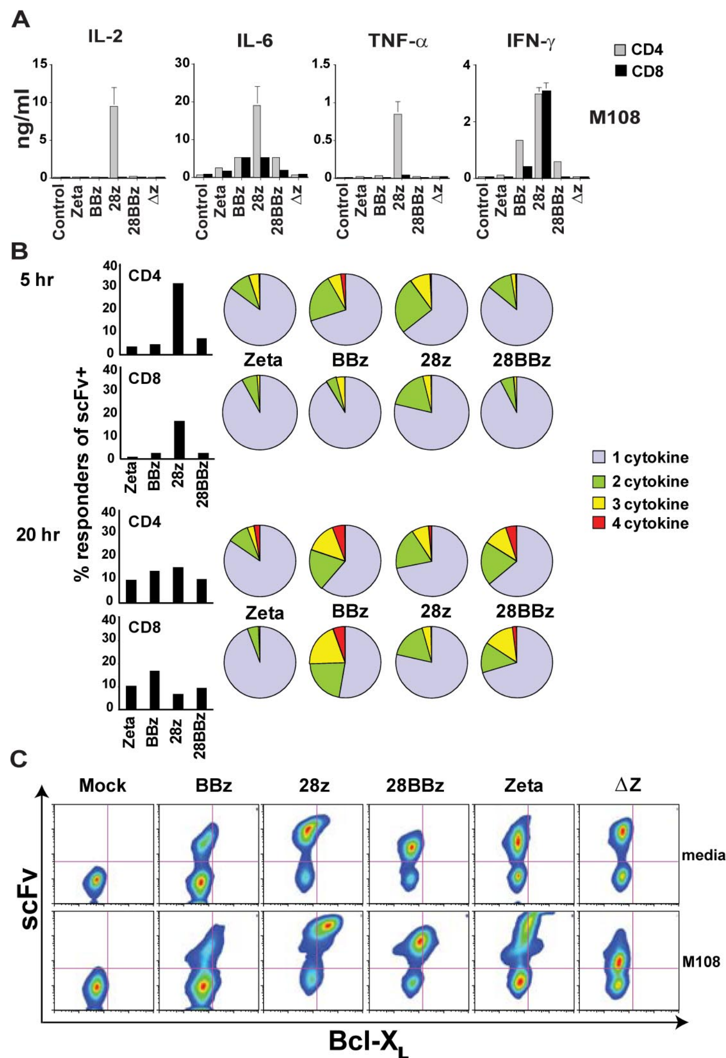

Fig. S2. Effects of costimulatory domains on cytokine production and Bcl-X_L expression in vitro. (*A*) The ability of transduced T cells to secrete cytokines upon antigen recognition was examined in vitro. Transduced CD4 or CD8 T cells, normalized to 50% chimeric receptor expression for all receptors, were combined with irradiated M108 cells. Supernatants were collected 24 h later and analyzed for cytokines using a cytometric bead array. Results are expressed as means and standard deviation of triplicates and are representative of 2 separate donors. Transduced T cells cultured in medium only or with mesothelin-negative tumor cells did not secrete detectable amounts of cytokines (not shown). (*B*) Individual cells were examined for their ability to produce multiple cytokines upon SS1 scFv:mesothelin recognition. Transduced CD4 and CD8 T cells were combined with M108 cells (2:1 ratio) for 5 h or 20 h (last 4 h in the presence of monensin) and stained for surface expression of SS1 scFv, CD4, and CD8, followed by intracellular staining for IFN-γ, TNF-α, IL-2, and GM-CSF. Transduced T cells producing each cytokine were enumerated, with the frequency of cells capable of any cytokine response shown in bar graphs. Boolean gating was also done to examine all possible combinations of cytokine response patterns and plotted in the pie charts. (*C*) Bcl-X_L expression was examined for SS1 scFv-transduced CD8 T cells after 20-h culture in media alone or with M108.

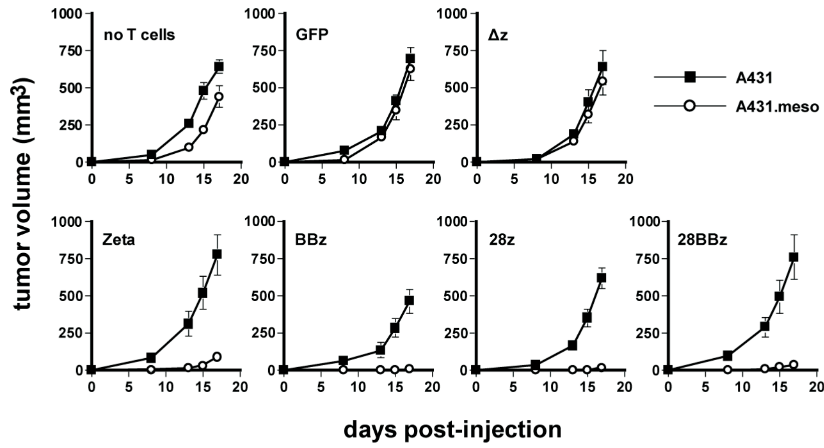

Fig. S3. Specificity of SS1 chimeric receptor transduced T cells in vivo. Rag2$\gamma^{-/-}$ mice were injected s.c. on opposite flanks with either 1×10^6 A431.meso or A431 parental tumor cells. Then, 5×10^5 T cells were coinjected with the tumor cells in each flank resulting in a 1:2 E:T ratio. The T cells were transduced with SS1 chimeric receptors expressing the indicated signaling domain; the transduction efficiencies were GFP 99%, Zeta 93%, BBz 69%, 28z 53%, 28BBz 66%, and Δz 70%. Results are represented as mean tumor volume (mm^3 +/– SD) with $n = 8$ for all groups, and are representative of 2 experiments.

A

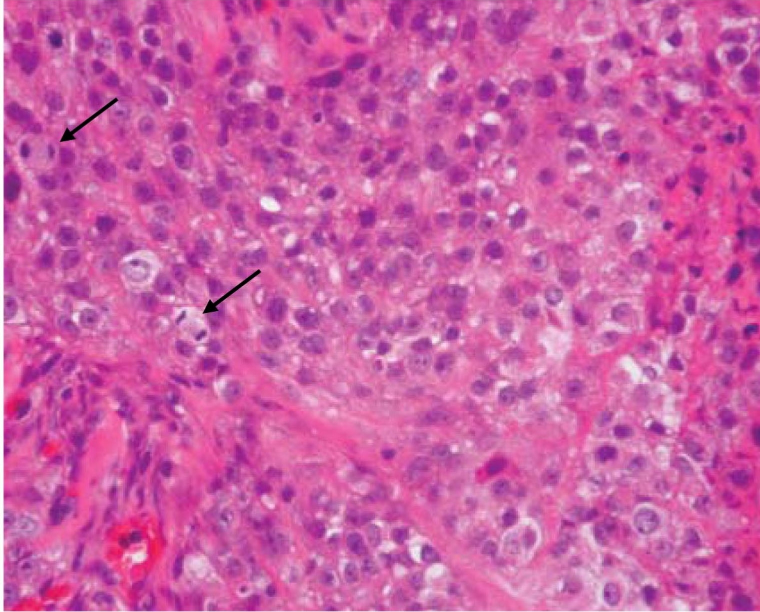

B

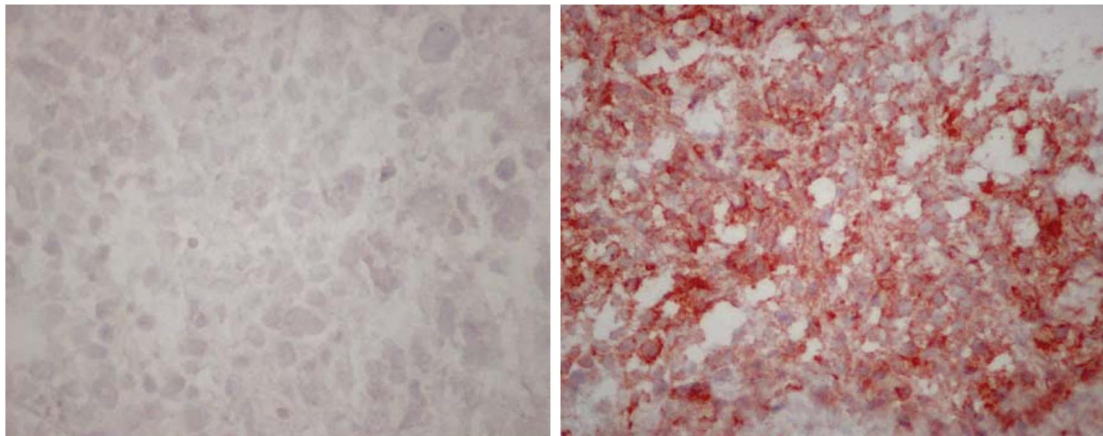

Fig. S4. In vivo mesothelin expression on M108 tumor xenograft. (*A*) M108 tumors were grown in NOG mice for ≈80 days, until they reached a volume of ≈2,000 mm^3, at which point the mice were killed. Portions of tumors were removed, embedded in paraffin, and sections were stained with hematoxylin and eosin. Cells undergoing mitosis are indicated by arrows. (*B*) Tumors were also embedded in OCT blocks and sections were stained for human mesothelin expression. All photographs were taken at 40× magnification.

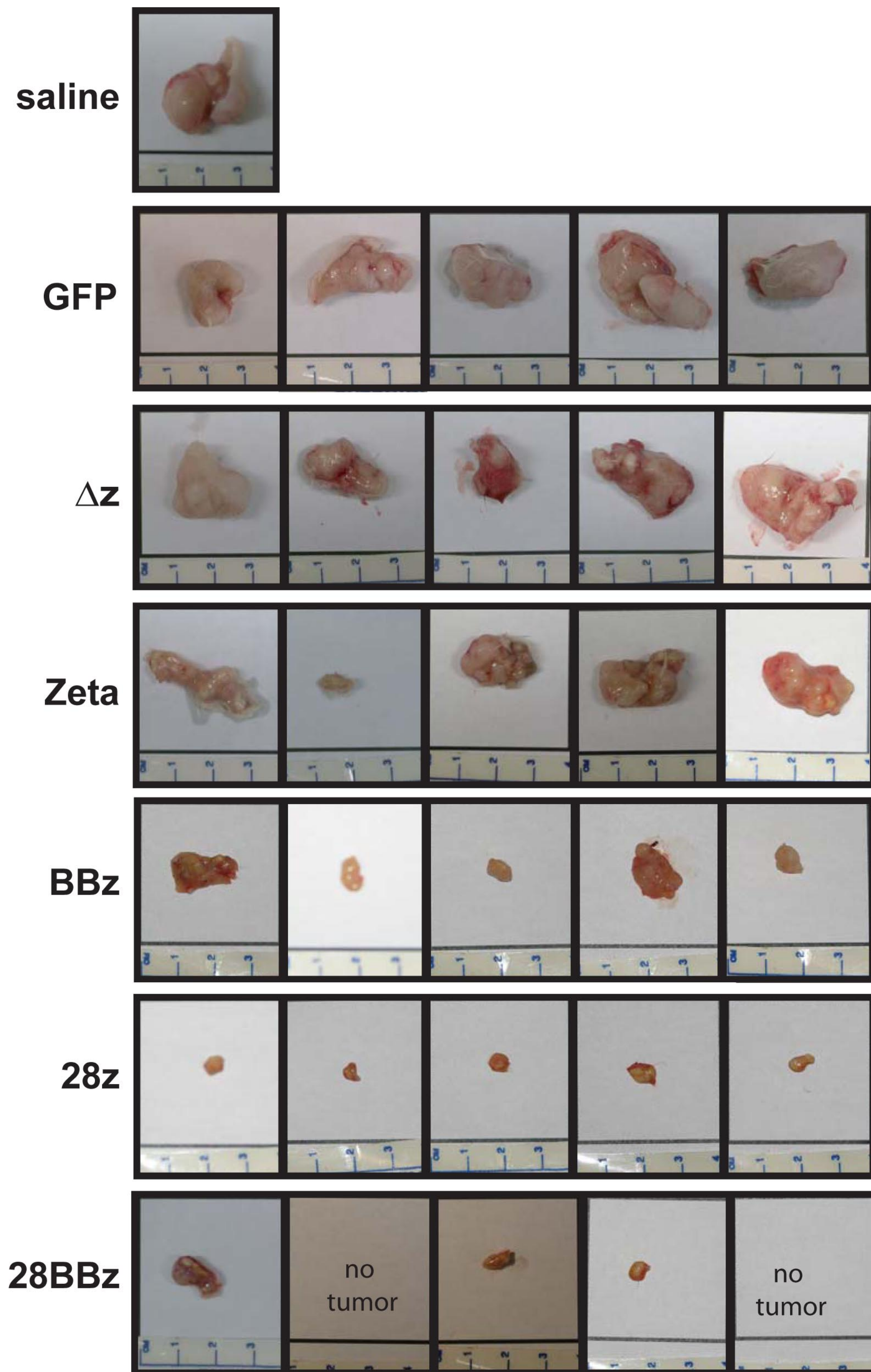

Fig. S5. M108 tumors after treatment with SS1-chimeric receptor transduced human T lymphocytes. Established M108 tumors in NOG mice were treated with intratumoral injections of SS1-CIR-transduced T lymphocytes on days 46 and 53 as described in Fig. 2*A*. Mice were killed when tumors reached volumes >2,000 mm^3 or when they displayed signs of distress, and tumors were photographed. Tumors from the saline, GFP, and Δz groups were removed on days 78 and 79 of the experiments. Tumors from the other groups were removed at later time points: Zeta (days 79, 80, 81, 88, 89), BBz (days 80, 89, 96), 28z (days 89, 96, 97), 28BBz (days 82, 89, 97). Only 1 representative tumor from a saline-treated animal is shown. Many of the small tissue masses harvested from the BBz, 28z, and 28BBz groups were largely fibrotic or necrotic masses, but they did contain small numbers of tumor cells with abnormal morphology (as confirmed by histology). Scale is shown in each photograph; ruler indicates 1-cm increments.